



**REVIEW**

# Malachite Green Adsorption Using Carbon-Based and Non-Conventional Adsorbent Made from Biowaste and Biomass: A Review

Annisa Ardiyanti, Suprpto Suprpto and Yatim Lailun Ni'mah\*

Department of Chemistry, Faculty of Sciences and Data Analytics, Institut Teknologi Sepuluh Nopember, Kampus ITS-Sukolilo, Surabaya, 60111, Indonesia

\*Corresponding Author: Yatim Lailun Ni'mah. Email: yatimnikmah@gmail.com

Received: 06 June 2023 Accepted: 24 July 2023 Published: 31 October 2023

## ABSTRACT

Dyes are pervasive contaminants in wastewater, posing significant health risks to both humans and animals. Among the various methods employed for effective dye removal, adsorption has emerged as a highly promising approach due to its notable advantages, including high efficiency, cost-effectiveness, low energy consumption, and operational simplicity compared to alternative treatments. This comprehensive review focuses on investigating adsorbents derived from biowastes and biomass, specifically carbon-based and non-conventional adsorbents, for the removal of malachite green, a widely used dye known for its toxic and carcinogenic properties. Carbon-based adsorbents encompass two main types: activated carbon and biochar, while non-conventional adsorbents refer to powder sorbents without carbonaceous treatments. Extensive studies have reported remarkable findings, with achieved maximum removal percentages exceeding 98% and capacities reaching 250 mg/g. These results highlight the exceptional efficacy of the reviewed adsorbents in eliminating malachite green from wastewater. By exploring the potential of bio-based adsorbents, this review sheds light on sustainable and environmentally friendly solutions for mitigating dye pollution.

## KEYWORDS

Adsorption; carbon; dyes; malachite green; wastewater

## 1 Introduction

In recent times, the rapid growth of industries has led to a prevalent environmental problem known as wastewater pollution. Wastewater contains a diverse range of contaminants, including household waste, pharmaceutical waste, metals, and dyes. Dyes, extensively utilized in industrial sectors such as paper, cosmetics, paint, leather tanning, and textiles, contribute significantly to the presence of wastewater. Among these sectors, the textile industry stands out, accounting for a substantial proportion of wastewater due to its high usage of dyes, surpassing other industries with a proportion of 54% compared to 21% for dyes, 10% for paper, and 8% for the paint industry [1].

The production of synthetic dyes exceeds 100,000 tons annually, with approximately  $7 \times 10^{-5}$  tons discharged into water each year [2]. While the dye industry plays a crucial role in economic growth, the discharge of dyes into water poses a significant risk to the ecosystem and the health of both animals and



humans. Dyes present in water impede sunlight penetration, thereby inhibiting the photosynthesis process of aquatic plants [3,4].

Among the numerous dyes used in industries, several possess hazardous characteristics and can harm living organisms upon release into the environment [5]. Malachite Green (MG), a widely employed basic-cationic dye in the textile industry, goes by various names such as basic green 4, aniline green, victoria green B, and diamond green B with its structure shown in Fig. 1 [6]. Its crystalline form appears as a dark green color, which transforms into a blue hue upon dissolution in water [7,8]. MG exhibits a pKa value ranging from 3.70 to 4.80 and demonstrates monoprotic Bronsted acid-base characteristics [9]. Within the textile industry, MG finds application in the dyeing of leather, wool, and silk. It possesses advantageous properties, such as antibacterial, antifungal, and antiparasitic effects, which are beneficial for aquaculture. Furthermore, it is a cost-effective dye that enjoys global availability. However, the well-documented harmful effects of MG on both humans and animals, including its carcinogenic, mutagenic, and teratogenic properties, have prompted its prohibition in several countries [10,11]. The permissible threshold for Malachite Green in water is set at 0.01 mg/L [12]. To mitigate these hazards, the removal of dyes from wastewater is of utmost importance.

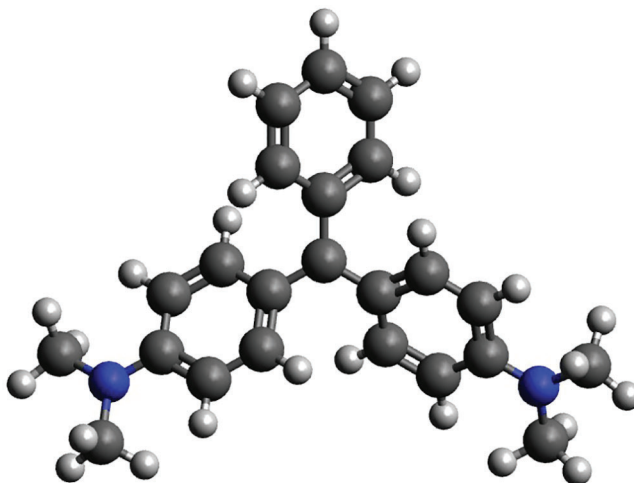


**Figure 1:** Malachite green structure

Methods for the removal of malachite green have been extensively studied and reported in the literature. These methods include photocatalytic processes [13–16], decolorization techniques [17–21], flocculation methods [22], and ozonation processes [23]. However, these approaches often suffer from drawbacks such as complicated operations and high costs.

In contrast, adsorption has emerged as an effective and widely utilized method for wastewater contaminant removal. It is renowned for its simplicity, cost-effectiveness, and high efficiency in removing contaminants. Adsorption involves two essential components: the adsorbate, referring to the material being adsorbed, and the adsorbent, responsible for the adsorption process. Various adsorbents have been employed, particularly in paper-based treatments, to target the removal of dyes [24,25].

Bio wastes have gained recognition as highly valuable resources for dye adsorption. These materials can be converted into powder or carbon-based adsorbents, such as activated carbon and biochar, through the utilization of acid or base as activating agents [26]. Activated carbon undergoes a chemical activation process that increases its pore size, while physical activation does not require the use of chemicals [27]. Biochar, on the other hand, is primarily produced through a high-temperature pyrolysis process [28,29]. Carbon-based adsorbents are characterized by their high porosity and large surface area [30]. Biosorbents, commonly used in powder form without carbonization processes, are another type of adsorbent [31,32]. Both carbon-based and biosorbents are cost-effective since they can be derived from plants and waste

materials readily available in our surroundings. In this paper, we aim to explore various adsorbents derived from biowastes and investigate their advantages in the specific removal of Malachite Green, a dye of particular interest [33–36].

## 2 Mechanisms of Adsorption

Adsorption occurs when the adsorbate and adsorbent surfaces reach equilibrium. This equilibrium is achieved through a series of steps known as the adsorption mechanism. The adsorption mechanism for dye onto its adsorbent typically involves four stages: (1) the transfer of the dye solution to the bulk adsorbent surface; (2) diffusion of the dye through the boundary layer to the adsorbent surface; (3) movement of the dye from the adsorbent surface to the interior pores; (4) adsorption occurring at the active sites of the adsorbent surface [37].

For cationic dyes like malachite green, the adsorption mechanisms may involve various processes such as electrostatic attraction, formation of hydrogen bonds, pore filling, n- $\pi$  interactions, and  $\pi$ - $\pi$  interactions [33]. These mechanisms contribute to the overall adsorption of the dye onto the adsorbent surface.

The adsorption mechanism of Malachite Green onto *Luffa aegyptica* peel adsorbent is influenced by the structure and surface properties of the adsorbate and adsorbent. Mashkoo et al. [38] conducted an analysis using FTIR and found that the adsorbent surface contains hydroxyl, carbonyl, and amine groups. They proposed that hydrogen bonding may occur between the hydroxyl groups on the adsorbent surface and the nitrogen atoms of Malachite Green. Additionally, electrostatic forces may play a role in the further adsorption of Malachite Green onto the negatively charged adsorbent surface [38].

Hydrogen bonding can occur between the hydrogens of the hydroxyl groups on the adsorbent surface and atoms such as nitrogen and oxygen. Moreover, hydrogen bonding can form between the OH<sup>-</sup> groups on the adsorbent surface and the aromatic rings of the cationic dye. In n- $\pi$  interactions, there are electron donors and acceptors, where the aromatic rings of the dye act as electron acceptors and the oxygens from the adsorbent carbonyl group act as electron donors [39].

Nethaji et al. [37] proposed that there is a reaction between the basic-cationic dye Malachite Green and a negatively charged adsorbent due to the presence of acidic functional groups. They observed a diffusive mass transfer followed by intraparticle diffusion, with intraparticle diffusion being higher for the basic dye compared to the acid dye during adsorption on acid-activated carbon.

To determine the predominant mechanism, two well-known models, Boyd's equation and Weber's pore diffusion model, can be employed. Boyd's equation is commonly used to assess intraparticle diffusion, and its derivative can provide insights into the different steps involved in the adsorption process. Boyd's equation is expressed as:

$$F = 1 - \left(\frac{6}{\pi^2}\right) \sum_{n=1}^{\infty} \left(\frac{1}{n^2}\right) \exp(-nBt) \quad (1)$$

$$F = \frac{q_t}{q_e} \quad (2)$$

where  $F$  is the fractional attainment of equilibrium, at different times,  $t$ ,  $Bt$  is a function of  $F$ ,  $q_t$ , and  $q_e$  are the dye uptake in mg/g. The determination of the rate of mass transfer in the adsorption process can be achieved through the analysis of  $Bt$  (a function of  $F$ ,  $q_t$ , and  $q_e$ ) plotted against time,  $t$ . If the plot is linear and passes through the origin, it indicates that pore diffusion is the controlling factor. However, if the plot is linear but does not pass through the origin, film diffusion is the rate-limiting step. This term is also applicable if the plot is nonlinear and does not pass through the origin [34].

Pathania et al. demonstrated a two-step adsorption mechanism for Malachite Green, as depicted in Fig. 2. The first step involves bulk diffusion across the surface, followed by surface adsorption. During the adsorption process, internal diffusion of the adsorbate controls the rate, as it is the slowest step, in accordance with Weber's intraparticle diffusion model [1]. Pathy et al. [40] also employed the intraparticle diffusion model in conjunction with the diffusion-chemisorption model to elucidate the adsorption process of Malachite Green on biochar. The obtained data indicated that both chemisorption and diffusion play crucial roles in the rate-determining step. At lower concentrations, the diffusion-chemisorption model provided an excellent fit. However, as the concentration increased, the  $R^2$  value significantly decreased, and the intraparticle diffusion (IPD) plot increased. This can be attributed to chemisorption not being the rate-determining step at higher Malachite Green concentrations, with diffusion becoming more prominent. At lower concentrations, particle interactions occur between the adsorbent surface and Malachite Green, leading to chemisorption as the dominant mechanism due to the low number of particles. At higher concentrations, saturation of Malachite Green particles occurs more rapidly [40].

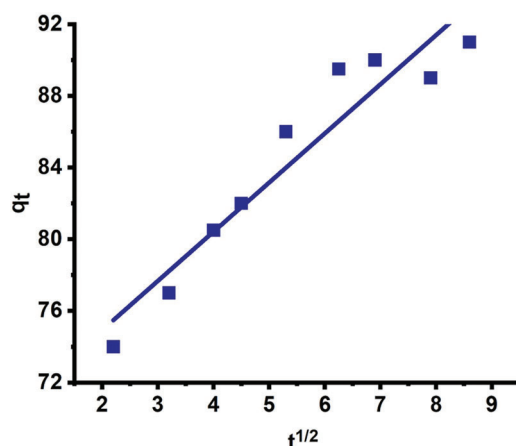


**Figure 2:** Intraparticle diffusion model for adsorption of malachite green on garlic peel

Adsorption can be classified into two types based on the interaction between the adsorbate and adsorbent: physisorption and chemisorption. Physisorption involves weak intermolecular forces, such as Van der Waals forces, resulting in non-chemical bond formation. Physisorption typically occurs as a multilayer adsorption and is exothermic, with energies below 40 kJ/mol. On the other hand, chemisorption involves higher energies (>40 kJ/mol), enabling the breaking and forming of chemical bonds. In chemisorption, the adsorbate molecules form specific chemical bonds with functional groups on the adsorbent surface, resulting in monolayer adsorption. Chemisorption can be either exothermic or endothermic [41–44]. Adsorption mechanism illustration is shown in Fig. 3.

### 3 Adsorbent from Waste Materials

Over time, waste materials have been widely employed for dye removal due to their cost-effectiveness and easy availability. Many researchers have explored numerous adsorbents for the removal of malachite green from synthetic wastewater. However, certain studies have also incorporated the use of real wastewater in their experiments to evaluate the effectiveness of adsorbents for malachite green removal. This includes the utilization of waste materials as well as other types of adsorbents. Table 1 provides examples of adsorbents used in real effluents, along with their corresponding results.

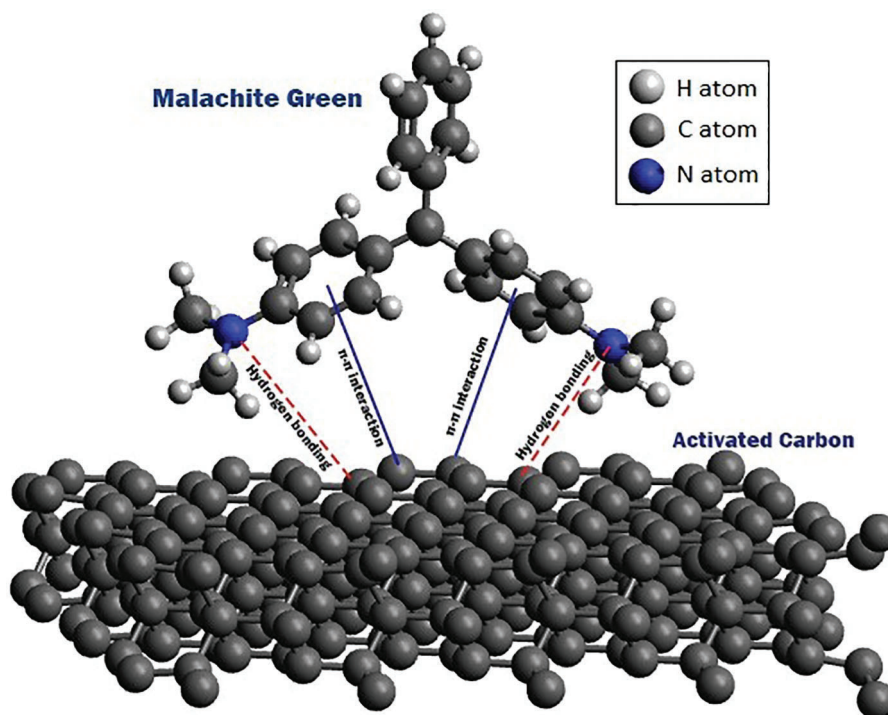


**Figure 3:** Illustration of adsorption mechanism

**Table 1:** Several materials used for malachite green removal

Adsorbent	Result	Ref.
Rice husk	Removal efficiency 96.96%	[45]
<i>Oscillatoria</i> sp	Removal efficiency 80%	[46]
Polymer inclusion membrane	Removal efficiency 98%	[47]

### 3.1 Carbon-Based

Carbon-based adsorbents have gained significant attention in recent years for the treatment of dye pollutants in wastewater. This category includes activated carbon, biochar, porous carbon, and carbon nanotubes. However, in this paper, our focus is specifically on activated carbon and biochar. The pore structure and surface area of carbon materials play a crucial role in their adsorption capacity, and there is often a positive correlation between the use of carbon-based adsorbents and enhanced adsorption capacity.

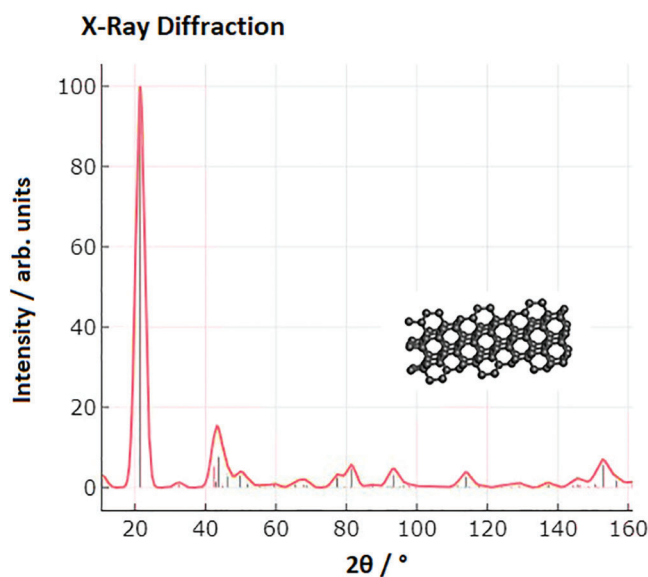
Activated carbon is commonly derived from biomass and undergoes a series of steps that involve washing and drying at specific temperatures. Activation can be achieved through physical or chemical processes [27]. Physical activation utilizes inert or oxidizing gases at temperatures ranging from 400°C to 900°C [48]. CO<sub>2</sub> gas is often used in physical activation to enhance the porosity of the carbon material [49]. Chemical activation, on the other hand, involves the use of activating agents such as NaOH, KOH, H<sub>2</sub>SO<sub>4</sub>, or ZnCl<sub>2</sub>. The carbon material is washed after heating and then mixed with the activating agent in a specific ratio. The role of the activating agent is to increase the active surface area by generating numerous pores and removing impurities [50].

Table 2 provides a summary of activated carbon produced from biowastes. For instance, Hameed et al. prepared bamboo-based activated carbon by crushing dried bamboo. The crushed material was impregnated with  $K_2CO_3$  as the activating agent in a 1:1 ratio and dehydrated overnight at  $105^\circ C$ . The dehydration process involved increasing the temperature three times under a nitrogen flow, followed by switching to carbon dioxide gas. The BET analysis revealed a surface area of  $1724\text{ m}^2/\text{g}$  and a pore volume of  $1.071\text{ cm}^3/\text{g}$  for the bamboo-based activated carbon. These favorable properties were achieved through the activation process involving  $K_2CO_3$  [34].

**Table 2:** Activated carbon adsorbents

AC source	Activator	Parameter				Removal (%)	q (mg/g)	Ref.
		Adsorbent dosage (g)	Dye concentration (mg/L)	Contact time (min)	pH			
Bamboo	$K_2CO_3$	–	25.00	20	4	98.60	263.58	[34]
Rambutan peel	KOH	–	25.00	180	8	92.00	–	[12]
Spent tea leaves	NaOH	0.020	–	–	4	94	256.40	[51]
Coconut coir	$ZnCl_2$	–	60.00	40	–	–	20.00	[52]
Durian seed	KOH	–	25.00	360	8	97.00	22.00	[53]
Oakwood	$HNO_3$	0.620	15.00	89	–	97.32	–	[54]
Elaeagnus	$ZnCl_2$	0.025	200.00	30	–	99.26	–	[55]
Chestnut shell	$ZnCl_2$	0.005	200.00	60	6	96	–	[56]
<i>Pinus roxburghii</i> cone	$CH_3COOH$	0.020	60.00	60	6	–	250.00	[36]
Coffee husk	$H_2SO_4$	0.025	–	120	6.8	–	264.81	[57]
<i>Amygdalus scoparia</i>	Thermal	0.027	19.89	75	7	100	–	[58]
Coconut shell	$H_3PO_4$	–	20	180	–	–	32.79	[59]
<i>Catha edulis</i>	NaOH	0.5	10	60	10	98.8	4.55	[60]
<i>Curcuma caesia</i>	Thermal	3	10	35	9	88	–	[61]
<i>Cetraria islandica</i>	$ZnCl_2$	–	70	80	9	93.46	–	[62]
Fig leaves	$H_3PO_4$	0.4	50	200	10	96.3	61.33	[63]
<i>Hevea brasiliensis</i> root	KOH	–	–	–	4	–	259.49	[64]
Coconut shell	$ZnCl_2$	–	20	180	–	–	39.68	[65]

Activated carbon derived from *Cetraria islandica* was prepared by drying the material in an oven for 24 h [62]. The dried *Cetraria islandica* was then ground, frozen, and sieved to obtain activated carbon.  $\text{ZnCl}_2$  was used as the activating agent in a 1:1 ratio for impregnation. The surface area of the activated carbon was determined by BET analysis and found to be  $394.417 \text{ m}^2/\text{g}$ . The pore distribution was predominantly in the micropore region. Fig. 4 shows standard XRD for activated carbon derived from biomaterials. The diffractogram shows a sharp peak at  $2\theta = 20^\circ$ , indicating a crystalline structure.



**Figure 4:** XRD pattern of activated carbon

Activated carbon produced from coconut shell exhibited a high adsorption capacity of  $39.682 \text{ mg/g}$ . The  $\text{ZnCl}_2$ -activated carbon displayed a larger surface area ( $544.66 \text{ m}^2/\text{g}$ ), as determined by BET analysis, compared to the carbon derived from *Cetraria islandica*. The enhanced surface area can be attributed to the presence of nitrogen gas during carbonization in a tubular furnace under a nitrogen atmosphere. Without the presence of nitrogen gas, re-condensation may occur, leading to incomplete pore opening and potentially lower surface area [65]. It is important to note that the source of biomass used for synthesizing carbon also influences the structural properties and adsorption capacity [66]. The diffractogram shows a sharp peak at  $2\theta = 20^\circ$ , indicating a crystalline structure.

*Curcuma caesia*-based activated carbon was obtained by heating powdered rhizome at  $550^\circ\text{C}$  for 5 h without any chemical treatment. This process resulted in a high removal efficiency of 96%, and the column adsorption capacity was determined to be  $38.16 \text{ mg/g}$  [61].

**Table 3:** Biochar adsorbents

Biochar source	Parameter					
	Adsorbent dosage (g)	Dye concentration (mg/L)	Contact time (min)	pH	Removal (%)	Ref.
Sugarcane bagasse	–	3000	51.89	7.5	99.99	[67]
<i>Opuntia ficus-indica</i> (OFI) cactus	0.06	100	–	4	99.26	[68]

(Continued)

Table 3 (continued)						
Biochar source	Parameter					
	Adsorbent dosage (g)	Dye concentration (mg/L)	Contact time (min)	pH	Removal (%)	Ref.
<i>Pinus patula</i> wood	2.7	–	60	10	99.7	[69]
Chinese fan palm seed	–	150	–	7	99.7	[70]
Rice husk	–	–	120	6	96.96	[45]
Crab shell	–	–	–	8	99.90	[71]
Algal	20	0.065	180	7	83.62	[40]
Algal-kombucha	20	0.075	180	7	84.62	

Another significant carbon-based adsorbent is biochar, which is summarized in Table 3. Biochar is typically produced through thermochemical conversions such as pyrolysis, gasification, hydrothermal carbonization, and torrefaction, from various biomass sources. During pyrolysis, in the absence of oxygen, the lignocellulosic components of biomass undergo depolymerization, fragmentation, and cross-linking reactions at specific temperatures. Gasification refers to the decomposition of the carbonaceous material into gaseous products, while the resulting char is known as biochar. Hydrothermal carbonization is a cost-effective process conducted at low temperatures (around 180°C–250°C). Torrefaction, also known as mild pyrolysis, involves heating biomass at 300°C under an inert atmosphere to remove oxygen, moisture, and carbon dioxide. This process modifies biomass properties such as particle size, moisture content, surface area, heating rate, and energy density [72].

Biochar often exhibits similar structural properties to activated carbon. For example, Giri et al. produced biochar from Chinese Fan Palm through pyrolysis at 500°C for 4 h, with the pyrolysis chamber filled with nitrogen gas to minimize ash formation [70]. The biochar demonstrated a BET surface area of 43.2530 m<sup>2</sup>/g and achieved 99.5% removal of malachite green dye. Biochar derived from sugarcane bagasse through pyrolysis at 400°C exhibited excellent removal efficiency (99.99%), with a BET surface area of 382.89 m<sup>2</sup>/g. Higher pyrolysis temperatures resulted in larger surface areas. Comparatively, biochar produced from plant waste generally displayed larger surface areas than biochar from animal waste under similar conditions, mainly due to the higher inorganic components present [67].

Rice husk-derived biochar was modified using hydrothermal auxiliary alkali. It underwent carbonization at 550°C, and the temperature in the hydrothermal process was increased to 130°C for 5 h. The modified biochar demonstrated a maximum adsorption capacity of 373.02 mg/g, while the BET surface area for the modified and non-modified biochar was 434.62 and 21.764 m<sup>2</sup>/g, respectively [45].

### 3.2 Non-Conventional

Non-conventional adsorbents are extensively used and derived from various materials. These materials are typically transformed into powder form from their original state, and in some cases, undergo chemical treatments and decomposition processes [44]. In the scope of this paper, our review will focus specifically on non-conventional adsorbents derived from biowastes. Table 4 provides a summary of the non-conventional adsorbents discussed in this review.

**Table 4:** Non-conventional adsorbents

Source	Parameter			Removal (%)	q (mg/g)	Ref.
	Adsorbent dosage (g)	Dye concentration (mg/L)	Contact time (min)			
<i>Scendesmus quadricauda</i>	0.004	6	69	6	73.49	– [73]
<i>Chlorella vulgaris</i>	0.004	6	90	6	91.61	–
Eggshell	0.300	388	–	6	–	243.2 [74]
Walnut shell	0.030	–	90	5	–	54.56 [75]
Maize stalk	0.050	10	–	6	–	11.77 [76]
Maize bagasse						46.56
Potato peel	0.250	50	210	8	–	32.39 [77]
<i>Solanum tuberosum</i> leaves			21		75	–
<i>Solanum tuberosum</i> stem	0.100	10	18	7	67	– [78]
<i>Limonia acidissima</i>	0.400	100	210	7	98.87	12.35 [79]
<i>Carica papaya</i> wood	0.060	10	–	–	–	52.63 [80]
Watermelon rind	–	200	60	–	95.2	– [81]

Lara-Vásquez et al. investigated the use of *Zea mays* stalk and bagasse as adsorbents for malachite green adsorption. The stalk and bagasse were dried, separated, and ground to obtain particle sizes ranging from 0.84 to 0.42 mm for adsorption purposes. The surface area of the stalk and bagasse adsorbents was determined to be 4.79 and 6.92 m<sup>2</sup>/g, respectively. The adsorption capacity of malachite green was measured to be 11.77 and 46.56 mg/g for the stalk and bagasse adsorbents, respectively. The pH of the solution was monitored during the adsorption process as it influences the surface charge of the adsorbent and the ionization of the dye molecules. The pH plays a role in the competition between hydrogen ions and adsorbate ions for the active sites on the adsorbent surface [76].

*Carica papaya* wood (CPW) was studied as an adsorbent by Rangabhasiyam et al. [80]. The wood material was cut into small pieces and dried in an oven for 24 h. The dried CPW pieces were then crushed, and a fraction with a size range of 100–200 µm was selected as the biosorbent. The adsorption capacity of CPW for malachite green removal was found to increase with increasing pH from 2 to 10, with the highest removal observed at an initial pH of 10.

Eggshells were size fractionated and washed with distilled water before being dried at room temperature for 24 h. The experiment was conducted under optimal conditions determined by Response Surface Method-Box Behnken Design. The optimum conditions were determined to be an adsorbent dosage of 0.3 g, an initial dye concentration of 388 mg/L, and a pH of 6, resulting in an adsorption capacity of 243.2 mg/g [74]. Walnut shells were soaked, washed, and then oven-dried. The dried walnut shells were crushed, blended, and sieved to obtain the desired particle size. The adsorption capacity for malachite green was measured to be 90.8 mg/g using an adsorbent dosage of 0.03 g [75].

## 4 Factors Influencing Adsorption

### 4.1 Effect of Adsorbent Dosage

The effect of adsorbent dosage is a critical factor in determining the adsorption capacity of Malachite Green. Fig. 5 illustrates that both activated carbon and non-conventional adsorbents are capable of adsorbing Malachite Green up to 99%. It is observed that as the adsorbent dosage increases, the adsorption capacity tends to decrease. However, the removal efficiency of Malachite Green increases with an increase in adsorbent dosage. This can be attributed to a higher adsorbent dosage providing a larger number of available active sites for the adsorption process. As a result, a smaller amount of contaminants can occupy a larger surface area of the adsorbent, leading to a higher removal efficiency. It is important to note that there is a certain dosage beyond which the adsorbent's efficacy decreases. At this point, the removal efficiency becomes insignificant, indicating that the adsorption process has reached its optimum condition [82,83]. Previous studies have reported optimum adsorbent dosages for carbon-based and non-conventional adsorbents ranging from 0.03 to 3 g.

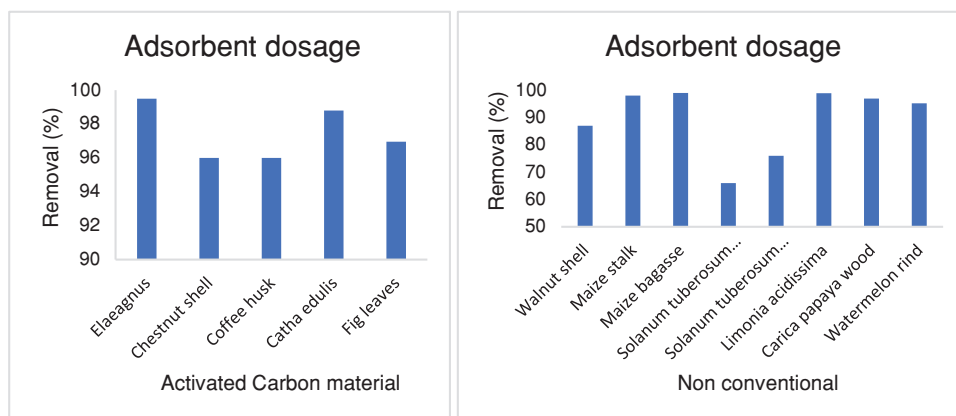


**Figure 5:** Comparison of activated carbon and non-conventional adsorbent

### 4.2 Effect of Dye Concentration

The initial dye concentration is another crucial parameter that significantly influences the adsorption process. Higher initial concentrations of the dye tend to result in lower removal percentages but higher adsorption capacities. This is because the active sites on the prepared adsorbent are surrounded by a larger amount of the adsorbate solution, leading to a higher capacity for adsorption [84]. An increase in the initial dye concentration enhances the diffusion of the dye particles from the bulk solution, facilitating the adsorption reaction and ultimately resulting in a higher adsorption capacity. However, it should be noted that adsorbents have limited active sites, and if these sites become saturated, the adsorption capacity decreases, leading to lower removal percentages [40]. Previous studies have reported that the optimum initial dye concentrations for carbon-based and non-conventional adsorbents, on average, were around 200 and 86.7 mg/L, respectively.

### 4.3 Effect of Contact Time

Contact time is a crucial parameter in the adsorption process as it determines the time required for the system to reach equilibrium. In studies on adsorption contact time, it has been observed that both the removal percentage and adsorption capacity increase with time until reaching equilibrium. At the beginning of the contact time, the mass transfer rate from the solution to the adsorbent is typically rapid. This is due to the availability of free surface area on the adsorbate and the pores of the adsorbent, facilitating the adsorption process [85]. Previous studies have reported an average optimum contact time of 110 min for carbon-based adsorbents and 96 min for non-conventional adsorbents.

#### 4.4 Effect of pH

The adsorption efficiency of adsorbents is influenced by the degree of ionization of the adsorbate molecules and the surface functional groups present. Conversely, the degree of ionization of the adsorbate molecules and the surface properties of the adsorbent are dependent on the pH of the solution. The pH of the solution plays a crucial role in bio-sorption studies as it affects the functional groups on the surface of the adsorbents and the chemical nature of the adsorbate, thereby influencing the adsorption behavior [86,87]. Previous studies have generally reported that the optimum pH for adsorption of Malachite Green and similar dyes falls within the neutral to alkaline range (pH 7–10) [58,60–63]. In alkaline pH conditions, increased protonation occurs, neutralizing the negative charges on the surface of the adsorbent and providing more active sites for adsorption [88]. Altering the pH can modify the physicochemical properties of both the adsorbate and the adsorbent. The removal rate of Malachite Green on activated carbon, for example, can be influenced by the reaction of the dye with H<sup>-</sup> and OH<sup>-</sup> ions present in the solution [89]. As shown in Fig. 6, carbon-based adsorbents demonstrate high adsorption capacities, with removal percentages exceeding 90% for Malachite Green dye.

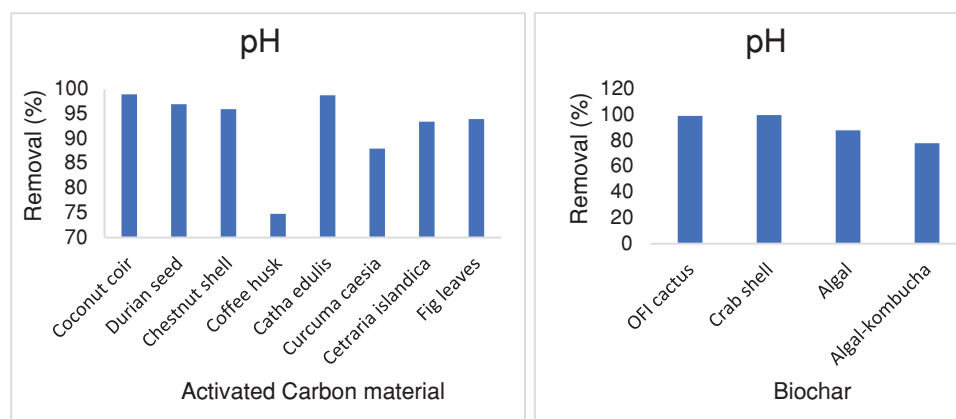


**Figure 6:** Comparison of carbon-based adsorbent

#### 5 Adsorbent Regeneration

Regeneration is a crucial aspect in determining the performance and sustainability of adsorbents for multiple adsorption cycles, as it minimizes the need for continuous production of new adsorbents and reduces solid waste accumulation. Desorption and thermal regeneration are commonly employed techniques for regenerating Malachite Green adsorbents [71]. Desorption involves the release of the previously adsorbed solution from the adsorbent and is widely used in the regeneration of Malachite Green adsorbents. To achieve effective regeneration through desorption, a suitable eluent is required to ensure high efficiency over multiple cycles. It is important to note that the adsorption capacity of the adsorbent may decrease after several cycles due to the reduction of exchangeable ions on the adsorbent surface and a decrease in active sites following regeneration [64,65]. For instance, You et al. reported a removal rate of 90.58% for Malachite Green after five cycles of desorption using HCl. The efficient desorption rate can be attributed to the protonation of H<sup>+</sup> in the solution, which interacts with the functional groups on modified rice husk and disrupts the structure of cellulose, providing new adsorption sites [90].

Thermal regeneration, on the other hand, does not involve the use of an eluent but instead relies on high temperatures. During thermal regeneration, the adsorbed dye is decomposed into small gas molecules that escape from the pore structure of the adsorbent [71]. In the isothermal reaction stages, a competitive

relationship between the deep carbonization process and the repair of adsorption/oxidation sites is observed. This relationship characterizes the regenerative behavior of the adsorbent [91]. The regeneration methods that have been studied for carbon-based and non-conventional adsorbent were summarized in Table 5.

**Table 5:** Regeneration methods for carbon-based and non-conventional adsorbent

Regeneration methods	Results	Ref.
Desorption in ethanol	Removal maintained at >90% after seven cycles	[1]
Desorption in 0.1 M HCl, NaOH, CH <sub>3</sub> COOH, and NaCl	Desorption efficiency >40% after four cycles	[38]
Desorption in ethanol	Adsorption efficiency for algal-biochar and algal-kombucha-biochar decreased from 84% to 81% and 8% to 84.5%	[40]
Desorption in acetone, pure methanol, methanol + 1% acetic acid, methanol + 3% acetic acid, and methanol + 5% acetic acid	Highest regeneration efficiency was 84% with methanol + 5% acetic acid. After seven cycles, 78% part of the Malachite Green adsorbed onto the activated carbon	[56]
Desorption in acetonitrile, chloroform, 0.1 M HCl, 0.1 M H <sub>2</sub> SO <sub>4</sub> , 1 M glacial acetic acid, ethanol	Adsorption percentage decreased to 68.57% after five cycles	[67]
Thermal regeneration at 800°C	High removal (99%) after five cycles	[71]
Desorption in HNO <sub>3</sub> and NaOH	NaOH gave the best result, removal was maintained at 70% after five cycles with an adsorbent capacity around 40%	[75]
Desorption in 0.1 M HCl	Removal rate 90.58% after five cycles	[90]
Desorption in ethanol	Adsorbent capacity was 400–450 mg/g after five cycles	[92]
Desorption in ethanol	Removal percentage was 60.3% after three cycles	[93]
Desorption in methanol	Activated carbon capacity was 70.11 mg/g after five cycles, initial capacity was 106.72 mg/g	[94]
Desorption in 0.1 M HCl, NaOH, ethanol 95%	Adsorption capacity decreased to 30.85% after 4 cycles	[95]
Thermal regeneration in an inert atmosphere and activation by CO <sub>2</sub>	Adsorption capacity is always 100%	
Desorption in 0.1 M CH <sub>3</sub> COOH	Removal percentage was 50% after two cycles	[96]
Desorption in 0.1 N NaOH	97% regeneration efficiency after five cycles	[97]
Desorption in methanol	Removal efficiency was 68% after four cycles	[98]
Thermal regeneration, heated in oven for 12 h and tube furnace from room temperature to 300°C at a rate 5°C/min	Adsorption capacity decreased from 210.18 to 148.51 mg/g after 3 cycles and efficiency was 70.66%	[99]
Desorption in distilled water, 0.1 M HNO <sub>3</sub> , 0.1 M NaOH	80% removal with NaOH, 30% with HNO <sub>3</sub> , and 20% with distilled water all after 5 cycles	[100]

## 6 Conclusion

In conclusion, both carbon-based and non-conventional adsorbents have demonstrated high efficiency in the removal of malachite green and other dyes, indicating their potential for application in adsorption-based wastewater treatment methods. The studies reviewed in this manuscript have consistently shown that these adsorbents exhibit remarkable adsorption efficiency and capacity for malachite green removal. The adsorption process for malachite green is influenced by various factors, including adsorbent dosage, dye concentration, contact time, and pH. Optimizing these parameters is crucial for achieving maximum adsorption efficiency and capacity.

However, it is important to note that the majority of the studies reviewed were conducted on a laboratory scale, limiting our understanding of how these adsorbents would perform under large-scale or industrial conditions. Further research is required to assess the practical applicability and performance of these adsorbents when used directly in real-world wastewater treatment scenarios. These studies should consider the complexities of wastewater matrices and the potential presence of coexisting pollutants, which can impact the adsorption process.

Furthermore, it is necessary to investigate the regeneration potential and reusability of these adsorbents to ensure their sustainability and cost-effectiveness in long-term wastewater treatment applications. Overall, while the findings presented in this review highlight the promising potential of carbon-based and non-conventional adsorbents for malachite green removal, further research on a larger scale is essential to validate their performance and suitability for industrial wastewater treatment. These advancements will contribute to the development of efficient and sustainable methods for addressing dye pollution in wastewater.

**Acknowledgement:** The authors gratefully acknowledge financial support from the Institut Teknologi Sepuluh Nopember for this work, under the Project Scheme of the Publication Writing and IPR Incentive Program (PPHKI) 2024.

**Funding Statement:** The authors received no specific funding for this study.

**Author Contributions:** The authors confirm contribution to the paper as follows: study conception and design: Yatim Lailun Ni'mah and Suprpto Suprpto; data collection: Annisa Ardiyanti; analysis and interpretation of results: Yatim Lailun Ni'mah and Suprpto Suprpto; draft manuscript preparation: Annisa Ardiyanti. All authors reviewed the results and approved the final version of the manuscript.

**Availability of Data and Materials:** The authors confirm that the data supporting the findings of this study are available within the article.

**Conflicts of Interest:** The authors declare that they have no conflicts of interest to report regarding the present study.

## References

1. Pathania, D., Bhat, V. S., Shivanna, J. M., Sriram, G., Kurkuri, M. et al. (2022). Garlic peel based mesoporous carbon nanospheres for an effective removal of malachite green dye from aqueous solutions: Detailed isotherms and kinetics. *Spectrochimica Acta Part A: Molecular and Biomolecular Spectroscopy*, 276, 121197.
2. Soltani, M., Farammarzi, M., Mousavi Parsa, S. A. (2021). A review on adsorbent parameters for removal of dye products from industrial wastewater. *Water Quality Research Journal*, 5(4), 181–193.
3. Márquez, C. O., García, V. J., Guaypatin, J. R., Fernández-Martínez, F., Ríos, A. C. (2021). Cationic and anionic dye adsorption on a natural clay composite. *Applied Sciences*, 11(11), 5127.
4. Shi, Y., Chang, Q., Zhang, T., Song, G., Sun, Y. et al. (2022). A review on selective dye adsorption by different mechanisms. *Journal of Environmental Chemical Engineering*, 10(6), 108639.

5. Lellis, B., Fávaro-Polonio, C. Z., Pamphile, A. J., Poloni, J. C. (2019). Effects of textile dyes on health and the environment and bioremediation potential of living organisms. *Biotechnology Research and Innovation*, 3(2), 275–290.
6. Chain, E. F. S. A. (2016). Malachite green in food. *EFSA Journal*, 14(2), e04530.
7. Li, C., Kong, D., Yao, X., Ma, X., Wei, C. et al. (2022). Adsorption characteristics and molecular simulation of malachite green onto modified distillers' grains. *Water*, 14(2), 171.
8. Srivastava, S., Sinha, R., Roy, D. (2004). Toxicological effects of malachite green. *Aquatic Toxicology*, 66(3), 319–329.
9. Apolônio, L., Oliveira, A. F., Almeida, C. A., Neves, A., Queiroz, M. et al. (2020). Direct determination of malachite green and leucomalachite green in natural waters by exploiting solid-phase sorption and digital image. *Orbital*, 12, 193–204.
10. Deniz, F., Kepekci, R. A. (2017). Bioremoval of malachite green from water sample by forestry waste mixture as potential biosorbent. *Microchemical Journal*, 132, 172–178.
11. Yonel, S. H., Nasra, E., Oktavia, B., Etika, S. B. (2021). Optimasi penyerapan zat warna malachite green menggunakan karbon aktif dari kulit pisang kepok (*Musa balbisiana Colla*). *Periodic*, 10(2), 28–32.
12. Oguzie, E., Akalezi, C., Enenebaku, C., Aneke, J. (2010). Corrosion inhibition and adsorption behavior of malachite green dye on aluminum corrosion. *Chemical Engineering Communications*, 198, 46–60.
13. Lavand, A. B., Bhatu, M. N., Malghe, Y. S. (2019). Visible light photocatalytic degradation of malachite green using modified titania. *Journal of Materials Research and Technology*, 8(1), 299–308.
14. Mostafa, E. M., Amdeha, E. (2022). Enhanced photocatalytic degradation of malachite green dye by highly stable visible-light-responsive Fe-based tri-composite photocatalysts. *Environmental Science and Pollution Research*, 29(46), 69861–69874.
15. Gouasmia, A., Zouaoui, E., Mekkaoui, A. A., Haddad, A., Bousba, A. (2022). Highly efficient photocatalytic degradation of malachite green dye over copper oxide and copper cobaltite photocatalysts under solar or microwave irradiation. *Inorganic Chemistry Communications*, 145, 110066.
16. Tiwari, N., Chakraborty, S., Samal, K., Moulick, S., Mohapatra, B. G. et al. (2023). Photocatalytic degradation of malachite green using TiO<sub>2</sub> and ZnO impregnated on fecal sludge derived biochar. *Journal of the Taiwan Institute of Chemical Engineers*, 145, 104800.
17. Alaya, V., Kоди, R. K., Ninganna, E., Gowda, B., Shivanna, M. B. (2021). Decolorization of malachite green dye by *Stenotrophomonas maltophilia* a compost bacterium. *Bulletin of the National Research Centre*, 45(1), 81.
18. Qiao, W., Liu, H. (2019). Enhanced decolorization of malachite green by a magnetic graphene oxide-CotA laccase composite. *International Journal of Biological Macromolecules*, 138, 1–12.
19. Himanshu, Chamoli, S., Singh, A., Kapoor, R. K., Singh, S. et al. (2023). Purification and characterization of laccase from *Ganoderma lucidum* and its application in decolorization of malachite green dye. *Bioresource Technology Reports*, 21, 101368.
20. Xie, Y., Huang, J., Dong, H., Wu, T., Yu, L. et al. (2020). Insight into performance and mechanism of tea polyphenols and ferric ions on reductive decolorization of malachite green cationic dye under moderate conditions. *Journal of Environmental Management*, 261, 110226.
21. Yildirim, N. C., Tanyol, M., Yildirim, N., Serdar, O., Tatar, S. (2018). Biochemical responses of *Gammarus pulex* to malachite green solutions decolorized by *Coriolus versicolor* as a biosorbent under batch adsorption conditions optimized with response surface methodology. *Ecotoxicology and Environmental Safety*, 156, 41–47.
22. Liu, B., Lu, H., Wu, S., Wang, Z., Feng, L. et al. (2022). Octopus tentacle-like molecular chains in magnetic flocculant enhances the removal of Cu(II) and malachite green in water. *Separation and Purification Technology*, 282, 120139.
23. Zhou, X. J., Guo, W. Q., Yang, S. S., Zheng, H. S., Ren, N. Q. (2013). Ultrasonic-assisted ozone oxidation process of triphenylmethane dye degradation: Evidence for the promotion effects of ultrasonic on malachite green decolorization and degradation mechanism. *Bioresource Technology*, 128, 827–830.
24. Jiang, S., Xi, J., Deng, H., Dai, G., Fang et al. (2020). Low-cost and high-wet-strength paper-based lignocellulosic adsorbents for the removal of heavy metal ions. *Industrial Crops and Products*, 158, 112926.

25. Jiang, S., Xi, H., Dai, X., H., Wu, W. (2023). Easily-manufactured paper-based materials with high porosity for adsorption/separation applications in complex wastewater. *Frontiers of Chemical Science and Engineering*, 17, 830–839.
26. Jabar, J. M., Owakotomo, I. A., Ayinde, Y. T., Alafabusuyi, A. M., Olagunju, G. O. et al. (2021). Characterization of prepared eco-friendly biochar from almond (*Terminalia catappa* L) leaf for sequestration of bromophenol blue (BPB) from aqueous solution. *Carbon Letters*, 31(5), 1001–1014.
27. Ukanwa, K., Patchigolla, K., Sakrabani, R., Anthony, E., Mandavgane, S. (2019). A review of chemicals to produce activated carbon from agricultural waste biomass. *Sustainability*, 11(22), 6204.
28. Manyà, J. J. (2012). Pyrolysis for biochar purposes: A review to establish current knowledge gaps and research needs. *Environmental Science & Technology*, 46(15), 7939–7954.
29. Chatterjee, R., Sajjadi, B., Chen, W. Y., Mattern, D. L., Hammer, N. et al. (2020). Effect of pyrolysis temperature on physicochemical properties and acoustic-based amination of biochar for efficient CO<sub>2</sub> adsorption. *Frontiers in Energy Research*, 8, 85.
30. Johnson, C. (2014). Advances in pretreatment and clarification technologies. In: *Comprehensive water quality and purification*, pp. 60–74. Waltham: Elsevier.
31. Dey, S., Veerendra, G. T. N., Phani Manoj, A. V., Anjaneya Babu, P. S. S. (2023). Performances of plant leaf biosorbents for biosorption of phosphorous from synthetic water. *Cleaner Materials*, 8, 100191.
32. Letechipia, J. O., González-Trinidad, J., Júnez-Ferreira, H. E., Bautista-Capello, C., Robles Rovero, C. O. et al. (2023). Removal of arsenic from semiarid area groundwater using a biosorbent from watermelon peel waste. *Heliyon*, 9(2), e13251.
33. Tran, H. N., You, S. J., Nguyen, T. V., Chao, H. P. (2017). Insight into the adsorption mechanism of cationic dye onto biosorbents derived from agricultural wastes. *Chemical Engineering Communications*, 204(9), 1020–1036.
34. Hameed, B. H., El-Khaiary, M. I. (2008). Equilibrium, kinetics and mechanism of malachite green adsorption on activated carbon prepared from bamboo by K<sub>2</sub>CO<sub>3</sub> activation and subsequent gasification with CO<sub>2</sub>. *Journal of Hazardous Materials*, 157(2), 344–351.
35. Ahmad, M. A., Alrozi, R. (2011). Removal of malachite green dye from aqueous solution using rambutan peel-based activated carbon: Equilibrium, kinetic and thermodynamic studies. *Chemical Engineering Journal*, 171(2), 510–516.
36. Sharma, G., Sharma, S., Kumar, A., Naushad, M., Du, B. (2019). Honeycomb structured activated carbon synthesized from *Pinus roxburghii* cone as effective bioadsorbent for toxic malachite green dye. *Journal of Water Process Engineering*, 32, 100931.
37. Nethaji, S., Sivasanny, A., Mandal, A. B. (2013). Adsorption isotherms, kinetics and mechanism for the adsorption of cationic and anionic dyes onto carbonaceous particles prepared from *Juglans regia* shell biomass. *International Journal of Environmental Science and Technology*, 10(2), 231–242.
38. Mashkoo, F., Nasar, A. (2019). Preparation, characterization and adsorption studies of the chemically modified *Luffa aegyptica* peel as a potential adsorbent for the removal of malachite green from aqueous solution. *Journal of Molecular Liquids*, 274, 315–327.
39. Tran, H. N., You, S. J., Chao, H. P. (2017). Fast and efficient adsorption of methylene green 5 on activated carbon prepared from new chemical activation method. *Journal of Environmental Management*, 188, 322–336.
40. Pathy, A., Krishnamoorthy, N., Chang, S. X., Paramasivan, B. (2022). Malachite green removal using algal biochar and its composites with kombucha SCOBY: An integrated biosorption and phycoremediation approach. *Surfaces and Interfaces*, 30, 101880.
41. Atkins, P., de Paula, J. (2010). *Physical chemistry*, 9th edition. New York: W. H. Freeman.
42. Adebayo, M. A., Jabar, J. M., Amoko, J. S., Openiyi, E. O., Shodiya, O. O. (2022). Coconut husk-raw clay-Fe composite: Preparation, characteristics and mechanisms of congo red adsorption. *Scientific Reports*, 12(1), 14370.
43. Paso, K. G. (2022). Constructing thermodynamic models of toxic metal biosorption. In: *Microbial biodegradation and bioremediation*, 2nd edition, pp. 109–143. Elsevier.
44. Dutta, S., Gupta, B., Srivastava, S. K., Gupta, A. K. (2021). Recent advances on the removal of dyes from wastewater using various adsorbents: A critical review. *Materials Advances*, 2(14), 4497–4531.

45. Tsai, C. Y., Lin, P. Y., Hsieh, S. L., Kirankumar, R., Patel, A. K. et al. (2022). Engineered mesoporous biochar derived from rice husk for efficient removal of malachite green from wastewaters. *Bioresource Technology*, 347, 126749.
46. Getachew, D., Suresh, A., Kamaraj, M., Ayele, A., Benor, S. (2022). Removal of malachite green and mixed dyes from aqueous and textile effluents using acclimatized and sonicated microalgal (*Oscillatoria* sp.) biosorbents and process optimization using the response surface methodology. *International Journal of Phytoremediation*, 24(8), 881–892.
47. Ling, Y. Y., Mohd Suah, F. B. (2017). Extraction of malachite green from wastewater by using polymer inclusion membrane. *Journal of Environmental Chemical Engineering*, 5(1), 785–794.
48. Husien, S., El-taweel, R. M., Salim, A. I., Fahim, I. S., Said, L. A. et al. (2022). Review of activated carbon adsorbent material for textile dyes removal: Preparation, and modelling. *Current Research in Green and Sustainable Chemistry*, 5, 100325.
49. Dawood, S., Sen, T. (2014). Review on dye removal from its aqueous solution into alternative cost effective and non-conventional adsorbents. *Journal of Chemical and Process Engineering*, 1(104), 1–11.
50. Chiu, Y. H., Lin, L. Y. (2019). Effect of activating agents for producing activated carbon using a facile one-step synthesis with waste coffee grounds for symmetric supercapacitors. *Journal of the Taiwan Institute of Chemical Engineers*, 101, 177–185.
51. Akar, E., Altinişik, A., Seki, Y. (2013). Using of activated carbon produced from spent tea leaves for the removal of malachite green from aqueous solution. *Ecological Engineering*, 52, 19–27.
52. Uma, Banerjee, S., Sharma, Y. C. (2013). Equilibrium and kinetic studies for removal of malachite green from aqueous solution by a low cost activated carbon. *Journal of Industrial and Engineering Chemistry*, 19(4), 1099–1105.
53. Ahmad, M. A., Ahmad, N., Bello, O. S. (2014). Adsorptive removal of malachite green dye using durian seed-based activated carbon. *Water, Air, & Soil Pollution*, 225(8), 2057.
54. Hajati, S., Ghaedi, M., Yaghoubi, S. (2015). Local, cheap and nontoxic activated carbon as efficient adsorbent for the simultaneous removal of cadmium ions and malachite green: Optimization by surface response methodology. *Journal of Industrial and Engineering Chemistry*, 21, 760–767.
55. Geçgel, Ü., Üner, O., Gökara, G., Bayrak, Y. (2016). Adsorption of cationic dyes on activated carbon obtained from waste *Elaeagnus* stone. *Adsorption Science & Technology*, 34(9–10), 512–525.
56. Altintig, E., Onaran, M., Sari, A., Altundag, H., Tuzen, M. (2018). Preparation, characterization and evaluation of bio-based magnetic activated carbon for effective adsorption of malachite green from aqueous solution. *Materials Chemistry and Physics*, 220, 313–321.
57. Krishna Murty, T. P., Gowrishankar, B. S., Chandra Prabha, M. N., Kruthi, M., Hari Krishna, R. (2019). Studies on batch adsorptive removal of malachite green from synthetic wastewater using acid treated coffee husk: Equilibrium, kinetics and thermodynamic studies. *Microchemical Journal*, 146, 192–201.
58. Bagheri, R., Ghaedi, M., Asfaram, A., Alipanahpour Dil, E., Javadian, A. (2019). RSM-CCD design of malachite green adsorption onto activated carbon with multimodal pore size distribution prepared from *Amygdalus scoparia*: Kinetic and isotherm studies. *Polyhedron*, 171, 464–472.
59. Piriya, R. S., Jayabalakrishnan, R. M., Maheswari, M., Boomiraj, K., Oumabady, S. (2023). Comparative adsorption study of malachite green dye on acid-activated carbon. *International Journal of Environmental Analytical Chemistry*, 103(1), 16–30.
60. Abate, G. Y., Alene, A. N., Habte, A. T., Getahun, D. M. (2020). Adsorptive removal of malachite green dye from aqueous solution onto activated carbon of *Catha edulis* stem as a low cost bio-adsorbent. *Environmental Systems Research*, 9(1), 29.
61. Arora, C., Kumar, P., Soni, S., Mittal, J., Mittal, A. et al. (2020). Efficient removal of malachite green dye from aqueous solution using *Curcuma caesia* based activated carbon. *Desalination and Water Treatment*, 195, 341–352.
62. Koyuncu, H., Kul, A. R. (2020). Synthesis and characterization of a novel activated carbon using nonliving *lichen cetraria islandica* (L.) ach. and its application in water remediation: Equilibrium, kinetic and thermodynamic studies of malachite green removal from aqueous media. *Surfaces and Interfaces*, 21, 100653.

63. Gebreslassie, Y. T. (2020). Equilibrium, kinetics, and thermodynamic studies of malachite green adsorption onto Fig (*Ficus cartia*) leaves. *Journal of Analytical Methods in Chemistry*, 2020, 7384675.
64. Ahmad, A. A., Ahmad, M. A., Yahaya, N. K. E. M., Karim, J. (2021). Adsorption of malachite green by activated carbon derived from gasified *Hevea brasiliensis* root. *Arabian Journal of Chemistry*, 14(4), 103104.
65. Piriya, R. S., Jayabalakrishnan, R. M., Maheswari, M., Boomiraj, K., Oumabady, S. (2021). Coconut shell derived ZnCl<sub>2</sub> activated carbon for malachite green dye removal. *Water Science and Technology*, 83(5), 1167–1182.
66. Santoso, E., Ediati, R., Kusumawati, Y., Bahruji, H., Sulistiono, D. O. et al. (2020). Review on recent advances of carbon based adsorbent for methylene blue removal from waste water. *Materials Today Chemistry*, 16, 100233.
67. Vyavahare, G. D., Gurav, R. G., Jadhav, P. P., Patil, R. R., Aware, C. B. et al. (2018). Response surface methodology optimization for sorption of malachite green dye on sugarcane bagasse biochar and evaluating the residual dye for phyto and cytogenotoxicity. *Chemosphere*, 194, 306–315.
68. Choudhary, M., Kumar, R., Neogi, S. (2020). Activated biochar derived from opuntia ficus-indica for the efficient adsorption of malachite green dye, Cu<sup>+2</sup> and Ni<sup>+2</sup> from water. *Journal of Hazardous Materials*, 392, 122441.
69. Rubio-Clemente, A., Gutiérrez, J., Henao, H., Melo, A. M., Pérez, J. F. et al. (2021). Adsorption capacity of the biochar obtained from *Pinus patula* wood micro-gasification for the treatment of polluted water containing malachite green dye. *Journal of King Saud University-Engineering Sciences*. <https://doi.org/10.1016/j.jksues.2021.07.006>
70. Giri, B. S., Sonwani, R. K., Varjani, S., Chaurasia, D., Varadavenkatesan, T. et al. (2022). Highly efficient bio-adsorption of malachite green using Chinese fan-palm biochar (*Livistona chinensis*). *Chemosphere*, 287, 132282.
71. Wu, J., Yang, J., Feng, P., Wen, L., Huang, G. et al. (2022). Highly efficient and ultra-rapid adsorption of malachite green by recyclable crab shell biochar. *Journal of Industrial and Engineering Chemistry*, 113, 206–214.
72. Yaashikaa, P. R., Kumar, P. S., Varjani, S., Saravanan, A. (2020). A critical review on the biochar production techniques, characterization, stability and applications for circular bioeconomy. *Biotechnology Reports*, 28, e00570.
73. Kousha, M., Farhadian, O., Dorafshan, S., Soofiani, N. M., Bhatnagar, A. (2013). Optimization of malachite green biosorption by green microalgae—*Scenedesmus quadricauda* and *Chlorella vulgaris*: Application of response surface methodology. *Journal of the Taiwan Institute of Chemical Engineers*, 44(2), 291–294.
74. Podstawczyk, D., Witek-Krowiak, A., Chojnacka, K., Sadowski, Z. (2014). Biosorption of malachite green by eggshells: Mechanism identification and process optimization. *Bioresource Technology*, 160, 161–165.
75. Dahri, M. K., Kooh, M. R. R., Lim, L. B. L. (2014). Water remediation using low cost adsorbent walnut shell for removal of malachite green: Equilibrium, kinetics, thermodynamic and regeneration studies. *Journal of Environmental Chemical Engineering*, 2(3), 1434–1444.
76. Lara-Vásquez, E. J., Solache-Ríos, M., Gutiérrez-Segura, E. (2016). Malachite green dye behaviors in the presence of biosorbents from maize (*Zea mays L.*), their Fe-Cu nanoparticles composites and Fe-Cu nanoparticles. *Journal of Environmental Chemical Engineering*, 4(2), 1594–1603.
77. Guechi, E. K., Hamdaoui, O. (2016). Sorption of malachite green from aqueous solution by potato peel: Kinetics and equilibrium modeling using non-linear analysis method. *Arabian Journal of Chemistry*, 9, S416–S424.
78. Gupta, N., Kushwaha, A. K., Chattopadhyaya, M. C. (2016). Application of potato (*Solanum tuberosum*) plant wastes for the removal of methylene blue and malachite green dye from aqueous solution. *Arabian Journal of Chemistry*, 9, S707–S716.
79. Sartape, A. S., Mandhare, A. M., Jadhav, V. V., Raut, P. D., Anuse, M. A. et al. (2017). Removal of malachite green dye from aqueous solution with adsorption technique using *Limonia acidissima* (wood apple) shell as low cost adsorbent. *Arabian Journal of Chemistry*, 10, S3229–S3238.
80. Rangabhashiyam, S., Lata, S., B, P. (2018). Biosorption characteristics of methylene blue and malachite green from simulated wastewater onto carica papaya wood biosorbent. *Surfaces and Interfaces*, 10, 197–215.
81. Awokoya, K. N., Oninla, V. O., Adeyinka, G. C., Ajadi, M. O., Chidimma, O. T. et al. (2022). Experimental and computational studies of microwave-assisted watermelon rind–styrene based molecular imprinted polymer for the removal of malachite green from aqueous solution. *Scientific African*, 15, e01194.

82. Hema, M., Martin, P., Prasath, D., Arivoli, S. (2009). Adsorption of malachite green onto carbon prepared from borassus bark. *Arabian Journal for Science and Engineering*, 34(2A), 31–42.
83. Anbia, M., Ghaffari, A. (2011). Removal of malachite green from dye wastewater using mesoporous carbon adsorbent. *Journal of the Iranian Chemical Society*, 8(S1), S67–S76.
84. Gorzin, F., Bahri Rasht Abadi, M. (2018). Adsorption of Cr(VI) from aqueous solution by adsorbent prepared from paper mill sludge: Kinetics and thermodynamics studies. *Adsorption Science & Technology*, 36(1–2), 149–169.
85. Ahmad, T., Danish, M. (2022). A review of avocado waste-derived adsorbents: Characterizations, adsorption characteristics, and surface mechanism. *Chemosphere*, 296, 134036.
86. Ni'mah, Y. L., Subandi, A. P. K., Suprpto (2022). The application of silica gel synthesized from chemical bottle waste for zinc(II) adsorption using response surface methodology (RSM). *Heliyon*, 8(12), e11997.
87. Ni'mah, Y. L., Yuningsih, N., Suprpto (2023). The adsorption of Pb(II) using silica Gel synthesized from chemical bottle waste: Optimization using box-behnken design. *Journal of Renewable Materials*, 11(6), 2913–2924.
88. Al-Khazali, N., Al-Rubaey, E., Al-Da'amy, M., Kareem, E. (2017). Removal of malachite green from aqueous solution by Iraqi porcelanite rocks. *Journal of Global Pharma Technology*, 10(9), 150–156.
89. Qu, W., Yuan, T., Yin, G., Xu, S., Zhang, Q. et al. (2019). Effect of properties of activated carbon on malachite green adsorption. *Fuel*, 249, 45–53.
90. You, X., Zhou, R., Zhu, Y., Bu, D., Cheng, D. (2022). Adsorption of dyes methyl violet and malachite green from aqueous solution on multi-step modified rice husk powder in single and binary systems: Characterization, adsorption behavior and physical interpretations. *Journal of Hazardous Materials*, 430, 128445.
91. Jia, L., Cheng, P., Yu, Y., Chen, S. H., Wang, C. X. (2023). Regeneration mechanism of a novel high-performance biochar mercury adsorbent directionally modified by multimetal multilayer loading. *Journal of Environmental Management*, 326, 116790.
92. Chen, L., Mi, B., He, J., Li, Y., Zhou, Z. et al. (2023). Functionalized biochars with highly-efficient malachite green adsorption property produced from banana peels via microwave-assisted pyrolysis. *Bioresource Technology*, 376, 128840.
93. Brahma, D., Nath, H., Borah, D., Debnath, M., Saikia, H. (2022). Coconut husk ash fabricated CoAl-layered double hydroxide composite for the enhanced sorption of malachite green dye: Isotherm, kinetics and thermodynamic studies. *Inorganic Chemistry Communications*, 144, 109878.
94. Saygılı, H., Güzel, F. (2018). Usability of activated carbon with well-developed mesoporous structure for the decontamination of malachite green from aquatic environments: Kinetic, equilibrium and regeneration studies. *Journal of Porous Materials*, 25, 477–488.
95. Guo, F., Jiang, X., Li, X., Jia, X., Liang, S. et al. (2020). Synthesis of MgO/Fe<sub>3</sub>O<sub>4</sub> nanoparticles embedded activated carbon from biomass for high-efficient adsorption of malachite green. *Materials Chemistry and Physics*, 240, 122240.
96. Ghosh, K., Bar, N., Roymahapatra, G., Biswas, A. B., Das, S. K. (2022). Adsorptive removal of toxic malachite green from its aqueous solution by *Bambusa vulgaris* leaves and its acid-treated form: DFT, MPR and GA modeling. *Journal of Molecular Liquids*, 363, 119841.
97. Jabar, J. M., Adebayo, M. A., Odusote, Y. A., Yilmaz, M., Rangabhashiyam, S. (2023). Valorization of microwave-assisted H<sub>3</sub>PO<sub>4</sub>-activated plantain (*Musa paradisiacal* L) leaf biochar for malachite green sequestration: Models and mechanism of adsorption. *Results in Engineering*, 18, 101129.
98. Mallakpour, S., Sirous, F., Dinari, M. (2022). Bio-sorbent alginate/citric acid-sawdust/Fe<sub>3</sub>O<sub>4</sub> nanocomposite beads for highly efficient removal of malachite green from water. *International Journal of Biological Macromolecules*, 222, 2683–2696.
99. Yu, M., Han, Y., Li, J., Wang, L. (2017). CO<sub>2</sub>-activated porous carbon derived from cattail biomass for removal of malachite green dye and application as supercapacitors. *Chemical Engineering Journal*, 317, 493–502.
100. Mullick, A., Neogi, S. (2016). Synthesis of potential biosorbent from used stevia leaves and its application for malachite green removal from aqueous solution: Kinetics, isotherm and regeneration studies. *RSC Advances*, 6(70), 65960–65975.